Interference between $f_0(980)$ and $\rho(770)^0$ resonances in $B \to \pi^+\pi^- K$ decays

B. El-Bennich,[1] A. Furman,[2] R. Kamiński,[3] L. Leśniak,[3] and B. Loiseau[1]

[1]*Laboratoire de Physique Nucléaire et de Hautes Énergies (IN2P3-CNRS-Universités Paris 6 et 7), Groupe Théorie, Université Pierre et Marie Curie, 4 place Jussieu, 75252 Paris, France*

[2]*ul. Bronowicka 85/26, 30-091 Kraków, Poland*

[3]*Division of Theoretical Physics, The Henryk Niewodniczański Institute of Nuclear Physics, Polish Academy of Sciences, 31-342 Kraków, Poland*

(Received 18 August 2006; revised manuscript received 25 October 2006; published 13 December 2006)

We study the contribution of the strong interactions between the two pions in S and P waves to the weak $B \to \pi\pi K$ decay amplitudes. The interference between these two waves is analyzed in the $\pi\pi$ effective-mass range of the $\rho(770)^0$ and $f_0(980)$ resonances. We use a unitary $\pi\pi$ and $\bar{K}K$ coupled-channel model to describe the S-wave interactions and a Breit-Wigner function for the P-wave amplitude. The weak B-decay amplitudes, obtained from QCD factorization, are supplemented with charming penguin contributions in both waves. The four complex parameters of these long-distance terms are determined by fitting the model to the *BABAR* and Belle data on $B^{\pm,0} \to \pi^+\pi^- K^{\pm,0}$ branching fractions, CP asymmetries, $\pi\pi$ effective-mass and helicity-angle distributions. This set of data, and, in particular, the large direct CP asymmetry for $B^\pm \to \rho(770)^0 K^\pm$ decays, is well reproduced. The interplay of charming penguin amplitudes and the interference of S and P waves describes rather successfully the experimental $\mathcal{S}$ and $\mathcal{A}$ values of the CP-violating asymmetry for both $B^0 \to f_0(980)K^0_S$ and $B^0 \to \rho(770)^0 K^0_S$ decays.

DOI: 10.1103/PhysRevD.74.114009 PACS numbers: 13.25.Hw, 13.75.Lb

I. INTRODUCTION

Hadronic final-state interactions in three-body charmless B meson decays supply good opportunities for CP violation searches. In order to interpret in the most reliable way decay observables, it is necessary to take into account strong interaction effects between the produced meson pairs. These effects, at relative energies below and about 1 GeV, are clearly visible in the Dalitz plots of three-body weak decays such as $B \to \pi\pi K$ and $B \to \bar{K}KK$ [1–6]. In particular, one observes a distinct surplus of events at these relatively small effective masses distributed near the edge of the Dalitz plot. Prominent maxima are seen in the effective $\pi\pi$ mass distribution, notably the $f_0(980)$ and $\rho(770)^0$ resonances. Several resonances at higher energies are visible too, though their identification is less straightforward. The experimental effective-mass distributions of three-body B decays are extracted from Dalitz plots. One cannot describe these data without including final-state interactions. The values of branching ratios obtained in experimental analyses are model dependent. In phenomenological studies of B meson decays, the isobar model is employed, which has a large number of arbitrary phases and relative intensity parameters. It is important to use a well-constrained model to describe the final-state interactions, where the constraints can come from theory and analyses of other processes in which the same final states are produced. One of our aims is to reduce the number of free parameters by using a model which describes many resonances in a unitarized way.

In Ref. [7], particular attention was paid to the $B \to f_0(980)K$ channels which have relatively large branching ratios for charmless B decays. The amplitudes considered in [7], based on the QCD factorization approach, do not include hard-spectator and annihilation terms which contain phenomenological parameters. It was found that these amplitudes do not reproduce the $B^\pm \to f_0(980)K^\pm$ and $B^0 \to f_0(980)K^0$ branching ratios. Therefore, additional terms were included in the decay amplitudes in the form of long-distance contributions stemming from so-called charming penguins [8]. At the hadronic level, these contributions could be associated with intermediate $D_s^{(*)}D^{(*)}$ states and be understood as being part of the intricate final-state interactions in B decays. One can expect a sizable contribution from such processes as $B \to D_s^* D^{(*)}$ branching fractions are large. The addition of charming penguins and of $\pi\pi$ and $\bar{K}K$ coupled-channel final-state interactions in Ref. [7] allowed us to obtain a good agreement with the measured $B \to f_0(980)K$ branching ratios and to reproduce the effective $\pi\pi$ mass distribution of the *BABAR* and Belle data.

Long-distance contributions, similar to the charming penguin effects, have been considered by Cheng, Chua, and Soni [9]. Cheng, Chua, and Yang recently have studied the nature of the scalar mesons $f_0(980)$ and $a_0(980)$ in the decays $B \to f_0(980)K$, $B \to a_0(980)\pi$, and $B \to a_0(980)K$ using QCD factorization for the weak decay amplitudes [10]. Their calculations are for a $\bar{q}q$ state of the $f_0(980)$, but implications of a $q^2\bar{q}^2$ picture of the $f_0(980)$ are discussed also. In their work [10], however, they neither consider hadronic long-distance contributions nor pionic and kaonic final-state interactions.

In the literature, one finds different results on the relative size of the weak annihilation or hard-spectator contributions to the B-decay amplitude into two mesons [11–13]. A recent study in soft-collinear effective theory [11] concludes that the annihilation and chirally enhanced annihi-

lation contributions in charmless $B \to M_1 M_2$ decays are real to leading order in $\Lambda_{\rm QCD}/m_b$ (here M_1 and M_2 are nonisosinglet mesons, $\Lambda_{\rm QCD}$ is the QCD scale, and m_b the b-quark mass). These contributions constitute a small fraction of the experimentally determined total penguin amplitudes in the case $\bar{B}^0 \to K^- \pi^+$ or $B^- \to K^- \bar{K}^0$ decays and in the present work they are not considered. Even upon inclusion of the relatively small annihilation and hard-spectator contributions, the current QCD factorization results underestimate the average branching ratio for $B \to \rho K$ by a factor of 2 and larger [14,15] unless certain model parameters are strongly modified (see scenarios S2 to S4 in Ref. [15]). To be more quantitative, let us cite the branching ratio of the $B^- \to K^- \rho^0$ decay calculated by Leitner, Guo, and Thomas [14]. Including fully these two contributions, it is equal to 1.54×10^{-6}. This should be compared to the experimental branching ratio for this decay which lies between 3.9×10^{-6} and 5.1×10^{-6} with a typical error of 0.5×10^{-6} [1,4].

In this paper, we supplement the $B \to \rho(770)^0 K$, $\rho(770)^0 \to \pi^+ \pi^-$ decay amplitudes to the $B \to f_0(980) K$, $f_0(980) \to \pi^+ \pi^-$ amplitudes derived in Ref. [7]. The experimental branching ratio for the decay $B \to \rho(770)^0 K$ is of the same order of magnitude as for the $B \to f_0(980) K$ channel. A characteristic feature of the $B^\pm \to \rho(770)^0 K^\pm$ decay, however, is the very large value of the direct CP-violating asymmetry of about 0.3 measured by Belle [1] and *BABAR* [4]. The addition of the $B \to \rho(770)^0 K$ decay amplitudes enables us to study possible interferences between the S and P waves in $B \to \pi\pi K$ decays. These effects can be observed, in particular, in the time-dependent CP asymmetries of neutral B decays into $\rho(770)^0 K_S^0$ and $f_0(980) K_S^0$ channels. In $b \to s$ transitions, *new physics* contributions to these asymmetries have been put forward [16,17]. Nonetheless, one also should take into account the influence of meson-meson final-state interactions on these observables, among others on the deviation of the asymmetry parameter $\mathcal{S}$ from the standard model expectation value $\sin 2\beta$.

In Sec. II, after a concise summary of the S-wave contributions $B \to f_0(980) K$ of Ref. [7], we derive the $B \to \rho(770)^0 K$ decay amplitudes from the QCD factorization approach of Ref. [15]. We introduce a Breit-Wigner vertex function $\Gamma_{\rho\pi\pi}(m_{\pi\pi})$ in the $B \to \rho(770)^0 K$ decay amplitude to account for the $\pi\pi$ final-state interactions in the P wave. We complement this amplitude with the S-wave contribution $B \to f_0(980) K$ obtained in Ref. [7]. In Sec. III, we give our model expressions for the observables measured by the Belle and *BABAR* Collaborations. We briefly discuss our fitting method in Sec. IV. In Sec. V our results are compared to the experimental $\pi\pi$ mass and helicity-angle distributions, and we give our branching ratio values for $B \to \rho(770)^0 K$ and $B \to f_0(980)^0 K$ decays. We analyze the S- and P-wave interference effects as well as the influence of charming penguins on the CP-violating parameters $\mathcal{S}(m_{\pi\pi})$ and $\mathcal{A}(m_{\pi\pi})$ of the time-dependent asymmetry in neutral B^0 decays. Furthermore, we calculate the asymmetry parameters $\mathcal{S}$ and $\mathcal{A}$ and compare our results with experimental data. In Sec. VI, we summarize and propose further improvements of this work. Finally, for completeness, we give in the appendix the expressions of the $B^- \to f_0(980) K^-$ and $B^- \to (\pi^+ \pi^-)_{S-\rm wave} K^-$ decay amplitudes. This will also allow us to make a comparison with other approaches like that of Ref. [10].

II. AMPLITUDES FOR THE $B \to \pi\pi K$ DECAYS

A. A brief recall of the $B \to f_0(980) K$ amplitudes

In Ref. [7], the B decays into $\pi\pi K$ and $\bar{K}KK$ were studied for final-state $(\pi\pi)_S$ and $(\bar{K}K)_S$ pairs interacting in an isospin zero S wave from $\pi\pi$ threshold to about 1.2 GeV. The QCD factorization approach is the framework used to describe weak decays of B mesons into a quasi two-body state $f_0(980) K$. The effective coefficients $a_i(\mu) (i = 1, \ldots, 6)$ at the renormalization scale $\mu = 2.1$ GeV were taken from Ref. [18]. Corrections arising from annihilation topologies and hard-gluon scattering with the spectator quark were not included.

The two-pion and two-kaon rescattering effects are described by the $\pi\pi$ and $\bar{K}K$ unitary coupled-channel model of Ref. [19], which allows us to describe the lowest scalar-isoscalar resonances $f_0(600)$ and $f_0(980)$ with a single matrix of amplitudes. The meson-meson amplitudes are incorporated into four scalar form factors responsible for the production of the $\pi\pi$ and $\bar{K}K$ pairs in an isospin zero S wave from the current $\bar{u}u$, $\bar{d}d$, and $\bar{s}s$ antiquark-quark states. These scalar form factors are constrained by the chiral dynamics of low-energy meson-meson interactions [20] and provide the link between the weak decay amplitudes [18] and the hadronic rescattering model [19].

As mentioned in the introduction, charming penguin amplitudes were included. In a nutshell, these amplitudes are low-momentum $\bar{c}c$ loop contributions which are formally suppressed by powers of $\Lambda_{\rm QCD}/m_b$ though numerically enhanced by large Wilson coefficients [8]. No explicit calculations being available so far, one interprets these amplitudes as long-distance contributions parameterized by two complex parameters.

B. The $B \to \rho K$, $\rho \to (\pi\pi)_P$ decay amplitudes

The derivation of the $B \to \rho(770)^0 K$ weak decay amplitude follows the QCD factorization approach of Beneke and Neubert [15]. By $(\pi\pi)_P$ we denote isovector $\pi\pi$ states in a P wave and in the following we will write interchangeably $\rho(770)^0$ or $(\pi\pi)_P$ depending on the context. The possible quark line diagrams for negative B-meson decays are shown in Fig. 1, where the $\pi^+ \pi^-$ final-state interaction is graphically schematized by dashed lines appended to either a $\bar{u}u$ or $\bar{d}d$ state in the diagrams.

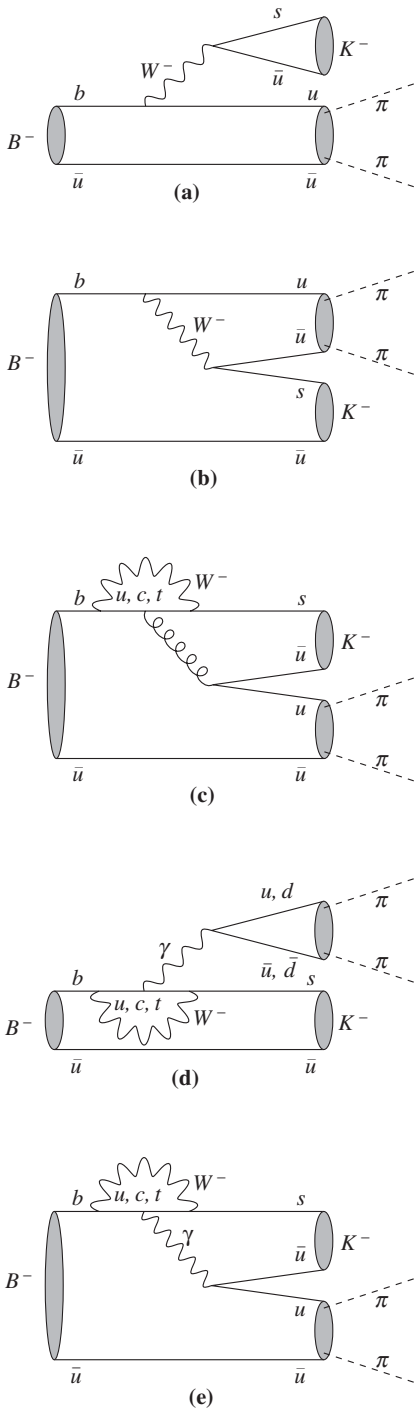

FIG. 1. Quark line diagrams for the B^- decay: (a) and (b) are tree diagrams, (c) is the penguin diagram, and (d) and (e) are electroweak penguin diagrams. The springlike lines represent gluon exchange, wavy lines photon or W^- exchange and the dashed ones the $\pi\pi$ isospin 1 P-wave pair.

The $B^- \to (\pi^+\pi^-)_P K^-$ decay amplitude can be written as

$$\langle(\pi^+\pi^-)_P K^-|H|B^-\rangle = p_K \cdot (p_{\pi^-} - p_{\pi^+}) A^- \Gamma_{\rho\pi\pi}(m_{\pi\pi}), \tag{1}$$

where p_K is four-momentum of K^- and p_{π^-} and p_{π^+} are the four-momenta of the negative and positive pions, respectively. In the $\pi^+\pi^-$ rest frame, the decay amplitude reduces to

$$\langle(\pi^+\pi^-)_P K^-|H|B^-\rangle = 2A^- \Gamma_{\rho\pi\pi}(m_{\pi\pi})|\mathbf{p}_\pi||\mathbf{p}_K|\cos\theta, \tag{2}$$

where $|\mathbf{p}_\pi|$ and $|\mathbf{p}_K| = \sqrt{E_K^2(m_{\pi\pi}) - M_K^2}$ are the moduli of the pion and kaon momenta with $E_K(m_{\pi\pi}) = \frac{1}{2} \times (M_B^2 - m_{\pi\pi}^2 - M_K^2)/m_{\pi\pi}$, M_B, $m_{\pi\pi}$, and M_K being the B meson, effective $\pi\pi$ and kaon masses, respectively. Moreover, θ is the helicity angle between the direction of flight of the π^- in the $\pi^+\pi^-$ rest frame and the direction of the $\pi^+\pi^-$ system in the B rest frame.

The function A^- is given by

$$A^- = G_F m_\rho [f_K A_0^{B\to\rho}(M_K^2)(U^- - C^P) + f_\rho F_1^{B\to K}(m_\rho^2) W^-], \tag{3}$$

where G_F is the Fermi coupling constant, $f_K = 159.8$ MeV is the kaon decay constant, and the ρ decay constant is given by $f_\rho = 209$ MeV. For the transition form factors $B \to \rho$ and $B \to K$, we employ $A_0^{B\to\rho}(M_K^2) = 0.37$ and $F_1^{B\to K}(m_\rho^2) = 0.34$, respectively. The above values for decay constants and transition form factors are taken from Table I of Ref. [15]. The functions U^- and W^- are defined as

$$U^- = \lambda_u[a_1 + a_4^u - a_4^c - r(a_6^u - a_6^c + a_8^u - a_8^c) + a_{10}^u - a_{10}^c] + \lambda_t[-a_4^c + r(a_6^c + a_8^c) - a_{10}^c] \tag{4}$$

and

$$W^- = \lambda_u a_2 - \lambda_t \frac{3}{2}(a_7 + a_9). \tag{5}$$

The chiral factor is given by $r = 2M_K^2/[(m_b + m_u)(m_s + m_u)]$, with $m_b = 4.46$ GeV and where $m_u = 5$ MeV and $m_s = 110$ MeV are the u- and s-quark masses, respectively. The coefficients $a_i(\mu = m_b/2)$ are taken to be the $a_{i,\mathrm{I}}(\pi K)$ of Table III in Ref. [21]. In Eq. (4), we did not include the annihilation contribution considered in Ref. [15]. The charming penguin contribution C^P in Eq. (3) is parameterized as

$$C^P = \lambda_u P_u + \lambda_t P_t, \tag{6}$$

with P_u and P_t being complex parameters [8]. In Eqs. (4)–(6), we have used the unitarity condition $\lambda_c + \lambda_u + \lambda_t = 0$, where $\lambda_u = V_{ub}V_{us}^*$, $\lambda_t = V_{tb}V_{ts}^*$, and $\lambda_c = V_{cb}V_{cs}^*$ are products of the Cabibbo-Kobayashi-Maskawa (CKM) matrix elements, to express the amplitudes in terms of λ_u and λ_t. The parameters of the CKM matrix are taken from Ref. [22].

The corresponding A^+ function of the $B^+ \to (\pi^-\pi^+)_P K^+$ decay amplitude is obtained from replacing the λ_u and λ_t values by their complex conjugates λ_u^* and λ_t^*

in Eqs. (4)–(6) and changing the overall sign in Eq. (2),

$$\langle(\pi^-\pi^+)_P K^+|H|B^+\rangle = 2A^+\Gamma_{\rho\pi\pi}(m_{\pi\pi})|\mathbf{p}_\pi||\mathbf{p}_K|\cos\theta, \tag{7}$$

where we define

$$A^+ = -A^-(\lambda_u^*, \lambda_t^*). \tag{8}$$

The minus sign in Eq. (8) follows from the CP symmetry of the final state.

Coming to neutral B decays, the $\bar{B}^0 \to \rho(770)^0\bar{K}^0$, $\rho^0 \to (\pi^+\pi^-)_P$ decay amplitude reads

$$\langle(\pi^+\pi^-)_P\bar{K}^0|H|\bar{B}^0\rangle = 2\bar{A}^0\Gamma_{\rho\pi\pi}(m_{\pi\pi})|\mathbf{p}_\pi||\mathbf{p}_K|\cos\theta, \tag{9}$$

with

$$\bar{A}^0 = G_F m_\rho[f_K A_0^{B\to\rho}(M_K^2)(\bar{U}^0 + C^P) + f_\rho F_1^{B\to K}(m_\rho^2)\bar{W}^0]. \tag{10}$$

The different sign in front of the charming penguin term C^P is due to the $\bar{d}d$ quark content of the $\rho(770)^0$ in neutral B decays in contrast to Eq. (3), where in charged B decays the $\bar{u}u$ configuration comes into play. The function $\bar{U}^0$ is given by

$$\bar{U}^0 = \lambda_u\{-a_4^u + a_4^c + r[a_6^u - a_6^c - (a_8^u - a_8^c)/2] + (a_{10}^u - a_{10}^c)/2\} + \lambda_t[a_4^c - r(a_6^c - a_8^c/2) - a_{10}^c/2] \tag{11}$$

and $\bar{W}^0 = W^-$. Here again we have left out annihilation contributions as considered in Ref. [15]. The replacement of λ_u and λ_t by their complex conjugate values in Eqs. (5) and (11) leads to the corresponding function A^0 for the $B^0 \to (\pi^-\pi^+)_P K^0$ decays which reads

$$\langle(\pi^-\pi^+)_P K^0|H|B^0\rangle = 2A^0\Gamma_{\rho\pi\pi}(m_{\pi\pi})|\mathbf{p}_\pi||\mathbf{p}_K|\cos\theta, \tag{12}$$

where one has again to account for an overall sign change in the amplitude

$$A^0 = -\bar{A}^0(\lambda_u^*, \lambda_t^*). \tag{13}$$

The $\rho \to \pi\pi$ vertex function is chosen to be of Breit-Wigner form,

$$\Gamma_{\rho\pi\pi}(m_{\pi\pi}) = \frac{g_{\rho\pi\pi}}{m_{\pi\pi}^2 - m_\rho^2 + i\Gamma_\rho m_\rho}, \tag{14}$$

where $m_\rho = 775.8$ MeV, the decay width is $\Gamma_\rho = 150.3$ MeV, and the coupling constant is taken to be $g_{\rho\pi\pi}^2/4\pi = 3m_\rho^2\Gamma_\rho/2p_\pi^3$.

C. Complete $B \to \pi\pi K$ decay amplitudes

We add the S-wave amplitude a_S of Ref. [7] for the $B \to (\pi\pi)_S K$ decays to obtain the complete decay amplitude as

$$\mathcal{M} = a_S + a_P|\mathbf{p}_\pi||\mathbf{p}_K|\cos\theta, \tag{15}$$

where a_S is given by either Eq. (1) or Eq. (7) of Ref. [7] and a_P can be read either from Eq. (2) or Eq. (9) for B^- decays or for $\bar{B}^0$ decays, respectively. The expression of the $B^- \to (\pi^+\pi^-)_S K^-$ amplitude can be found also in the appendix [Eq. (A12)]. It follows from Ref. [7] and from Eqs. (8) and (13) that the CP conjugate S- and P-wave amplitudes $\bar{a}_S$ and $\bar{a}_P$ are related to the amplitudes a_S and a_P by

$$\bar{a}_S = a_S(\lambda_u^*, \lambda_t^*), \qquad \bar{a}_P = -a_P(\lambda_u^*, \lambda_t^*). \tag{16}$$

Thus, the conjugate of $\mathcal{M}$ is written as

$$\bar{\mathcal{M}} = \bar{a}_S + \bar{a}_P|\mathbf{p}_\pi||\mathbf{p}_K|\cos\theta. \tag{17}$$

In the amplitude a_S of the present work, the charming penguin contribution $C(m)$ of Ref. [7] is replaced by

$$C^S(m) = -(M_B^2 - m^2)f_K F_0^{B\to(\pi\pi)_S}(M_K^2)(\lambda_u S_u + \lambda_t S_t). \tag{18}$$

In Eq. (18), S_u and S_t are two complex parameters and $F_0^{B\to(\pi\pi)_S}(M_K^2) = 0.46$ [7] is the B-transition form factor to a pair of pions in an S state. Furthermore, the constant χ, characteristic of the $f_0(980) \to \pi\pi$ decay, is fixed to 29.8 GeV^{-1} in agreement with the estimation made in Ref. [7]. Here, for the S wave, we also use the $a_{i,\mathrm{I}}(\mu = m_b/2)$ from Table III of Ref. [21] as effective coefficients a_i.

We can substitute the coefficients $a_i(PP)$ of the B decay into two pseudoscalar mesons PP in place of the coefficients $a_{i,\mathrm{I}}(PS)$ corresponding to the final pseudoscalar-scalar PS state for the following reasons. As can be seen from Eq. (35) of Ref. [15], the vertex corrections, which depend on the scalar light-cone distribution amplitudes, affect only the $a_{6,\mathrm{I}}(PS)$ coefficients of the amplitude for which the emitted meson without the quark spectator is a scalar. In our S-wave amplitude it is only found in the a_6 of Eq. (A5). However, $a_{6,\mathrm{I}}(PS)$ is practically equal to $a_{6,\mathrm{I}}(PP)$ (see Refs. [10] and [11] cited in Ref. [7]). Any further corrections to the a_i are due to hard-gluon scattering contributions ($a_{i,\mathrm{II}}(\mu)$ of Ref. [21]) as well as annihilation terms; both processes are, however, not included here.

III. DEFINITIONS OF OBSERVABLES

The $B \to \pi\pi K$ amplitude $\mathcal{M}$ in Eq. (15) depends on the effective-mass $m_{\pi\pi}$ and $\cos\theta$ which is equivalent to the other effective-mass variable $m_{\pi K}$ on the Dalitz plot. The double differential $B \to \pi\pi K$ decay distribution then reads

$$\frac{d^2\Gamma}{d\cos\theta dm_{\pi\pi}} = \frac{m_{\pi\pi}|\mathbf{p}_\pi||\mathbf{p}_K|}{8(2\pi)^3 M_B^3}|\mathcal{M}|^2. \tag{19}$$

Integrating over $\cos\theta$ one obtains the differential $B \to \pi\pi K$ decay distribution

$$\frac{d\Gamma}{dm_{\pi\pi}} = \frac{m_{\pi\pi}|\mathbf{p}_\pi||\mathbf{p}_K|}{4(2\pi)^3 M_B^3}\left(|a_S|^2 + \frac{1}{3}|\mathbf{p}_\pi|^2|\mathbf{p}_K|^2|a_P|^2\right), \tag{20}$$

and the differential branching ratio is given by

$$\frac{d\mathcal{B}}{dm_{\pi\pi}} = \frac{1}{\Gamma_B}\frac{d\Gamma}{dm_{\pi\pi}}, \tag{21}$$

where Γ_B is the appropriate total width for B^+ or B^0.

The integration on the Dalitz plot over the kinematically allowed $m_{\pi\pi}$ range yields the helicity-angle $B \to \pi\pi K$ distribution

$$\frac{d\Gamma}{d\cos\theta} = A + B\cos\theta + C\cos^2\theta. \tag{22}$$

The functions A, B, and C are defined as

$$A = \int_{m_{\min}}^{m_{\max}} \frac{m_{\pi\pi}|\mathbf{p}_\pi||\mathbf{p}_K|}{8(2\pi)^3 M_B^3}|a_S|^2 dm_{\pi\pi}, \tag{23}$$

$$B = 2\int_{m_{\min}}^{m_{\max}} \frac{m_{\pi\pi}|\mathbf{p}_\pi|^2|\mathbf{p}_K|^2}{8(2\pi)^3 M_B^3}\mathrm{Re}(a_S a_P^*) dm_{\pi\pi}, \tag{24}$$

$$C = \int_{m_{\min}}^{m_{\max}} \frac{m_{\pi\pi}|\mathbf{p}_\pi|^3|\mathbf{p}_K|^3}{8(2\pi)^3 M_B^3}|a_P|^2 dm_{\pi\pi}. \tag{25}$$

The CP-violating asymmetry for charged B decays is defined as

$$\mathcal{A}_{CP} = \frac{\frac{d\Gamma(B^- \to \pi^+\pi^- K^-)}{dm_{\pi\pi}} - \frac{d\Gamma(B^+ \to \pi^+\pi^- K^+)}{dm_{\pi\pi}}}{\frac{d\Gamma(B^- \to \pi^+\pi^- K^-)}{dm_{\pi\pi}} + \frac{d\Gamma(B^+ \to \pi^+\pi^- K^+)}{dm_{\pi\pi}}}. \tag{26}$$

Furthermore, in neutral B meson decays into final CP eigenstates f the time-dependent asymmetries are given by

$$\begin{aligned}\mathcal{A}_{CP}(t) &= \frac{\Gamma(\bar{B}^0(t) \to f) - \Gamma(B^0(t) \to f)}{\Gamma(\bar{B}^0(t) \to f) + \Gamma(B^0(t) \to f)} \\ &= \mathcal{S}\sin(\Delta m t) + \mathcal{A}\cos(\Delta m t).\end{aligned} \tag{27}$$

The mass difference between the two neutral B eigenstates is denoted by Δm, $\mathcal{S}$ is a measure for the mixing induced CP asymmetry, and $\mathcal{A}$ is the direct CP-violating asymmetry. The two parameters of the time-dependent asymmetry, $\mathcal{S}$ and $\mathcal{A}$, are

$$\mathcal{S} = \frac{2\,\mathrm{Im}\lambda_f}{1 + |\lambda_f|^2} = (1 - \mathcal{A})\,\mathrm{Im}\lambda_f, \tag{28a}$$

$$\mathcal{A} = -\frac{1 - |\lambda_f|^2}{1 + |\lambda_f|^2}, \tag{28b}$$

with

$$\lambda_f = e^{-2i\beta}\frac{\bar{\mathcal{M}}(\bar{B}^0 \to f)}{\mathcal{M}(B^0 \to f)} \tag{29}$$

and β being the CKM matrix angle. Inserting the corresponding amplitudes $\mathcal{M}(\bar{B}^0 \to f)$ from Eq. (15) and $\bar{\mathcal{M}}(B^0 \to f)$ from Eq. (17) into Eqs. (28a) and (28b), one obtains after integration over $\cos\theta$ the integrated $\mathcal{S}$ asymmetry

$$\begin{aligned}\mathcal{S}(m_{\pi\pi}) = (1 - \mathcal{A})2\,\mathrm{Im}\{e^{-2i\beta}[&\bar{a}_S a_S^* \\ &+ \tfrac{1}{3}|\mathbf{p}_\pi|^2|\mathbf{p}_K|^2\bar{a}_P a_P^*]\},\end{aligned} \tag{30}$$

and the $\mathcal{A}$ asymmetry integrated over $\cos\theta$ is

$$\mathcal{A}(m_{\pi\pi}) = \frac{|\bar{a}_S|^2 - |a_S|^2 + \frac{1}{3}|\mathbf{p}_\pi|^2|\mathbf{p}_K|^2(|\bar{a}_P|^2 - |a_P|^2)}{|\bar{a}_S|^2 + |a_S|^2 + \frac{1}{3}|\mathbf{p}_\pi|^2|\mathbf{p}_K|^2(|\bar{a}_P|^2 + |a_P|^2)}. \tag{31}$$

IV. FITTING PROCEDURE

In our fitting procedure we include the experimental data of Belle [1,3,23,24] and *BABAR* [4,5,25,26] collaborations. They include altogether 18 values of branching fractions, direct CP-violating asymmetries for the charged B decays, and the time-dependent CP asymmetry parameters $\mathcal{S}$ and $\mathcal{A}$ determined for the $B^0 \to \rho(770)K_S^0$ and $B^0 \to f_0(980)K_S^0$ decays. These data constitute the first part of the observable ensemble we fit. If one denotes by Z_i^{exp} and Z_i^{th} the experimental and theoretical value of the above mentioned observables and by $\Delta Z_i^{\mathrm{exp}}$ their empirical errors, then the corresponding first part of the χ^2 function reads:

$$\chi_{\mathrm{I}}^2 = W_{\mathrm{I}}\sum_{i=1}^{18}\left[\frac{Z_i^{\mathrm{exp}} - Z_i^{\mathrm{th}}}{\Delta Z_i^{\mathrm{exp}}}\right]^2. \tag{32}$$

Here, $W_{\mathrm{I}} = 10$ is a weight factor chosen so as to make a good balance between this and the second component χ_{II}^2 of the total χ^2 function. The χ_{II}^2 function is defined similarly to Eq. (32) but for the observables Z_i being the $\pi\pi$ effective-mass and the helicity-angle distributions. We set $W_{\mathrm{II}} = 1$. The experimental distributions have been background subtracted according to the figures of the Belle and *BABAR* papers cited above. For completeness, we give a list of figures showing the data we used in the evaluation of χ_{II}^2: Figs. 5b, 6c, 6d, and 7a through 7f from Ref. [23], Figs. 5c, 6c, and 6d from Ref. [3], Fig. 3b from Ref. [5], and Fig. 3 from Ref. [4]. The experimental data are not absolutely normalized; therefore, we have adopted an adequate method, described below, to compare the theoretical differential distributions of Eqs. (20) and (22) with the experimental $m_{\pi\pi}$ and $\cos\theta$ distributions.

For both differential distributions in $x = m_{\pi\pi}$ and $x = \cos\theta$, we define the theoretical number of events in a bin x_i by the integral

$$Y_{\rm th}(x_i) = \mathcal{N}\Gamma_B^{-1}\int_{x_{i1}}^{x_{i2}}\frac{d\Gamma(x)}{dx}dx. \quad (33)$$

The differential model distribution $d\Gamma(x)/dx$ is just that given by either Eq. (20) or Eq. (22) and the integration range of the kinematic variables is the bin width $[x_{i1}, x_{i2}]$. Then the normalization coefficient $\mathcal{N}$ of a given experimental distribution $Y_{\rm exp}$ is defined as a sum over all chosen bins:

$$\mathcal{N} = \Gamma_B\frac{\sum_{i=1}^{n} Y_{\rm exp}(x_i)}{\int_{X_1}^{X_2}\frac{d\Gamma(x)}{dx}dx}. \quad (34)$$

The sum of experimental events $Y_{\rm exp}(x_i)$ over x_i and the integration of $d\Gamma(x)/dx$ over x is done in the analyzed range $[X_1, X_2]$ of interest, which must be within the kinematically allowed range for the variables $m_{\pi\pi}$ and $\cos\theta$. Since we concentrate ourselves on the $\pi\pi$ effective-mass range where the $\rho(770)^0$ and $f_0(980)$ resonances contribute the most, we take in our fits $X_1 = 0.60$ GeV and $X_2 = 1.06$ GeV.

The experimental branching fractions for charged and neutral $B \to \rho(770)^0 K$ and $B \to f_0(980)K$ decays are obtained with the isobar model, in which the B-decay amplitude is a sum over the contributions of different two-body resonances. These are usually parameterized in terms of Breit-Wigner functions with the exception of the $f_0(980)$, for which the Flatté formula is used. After fitting the intensities of the resonances, a particular branching fraction for a given resonance is calculated as an integral over the fully available phase space on the Dalitz plot. In order to compare these experimental branching fractions with those for limited effective-mass ranges, we have calculated appropriate reduction coefficients as the ratio of the integral over the limited phase space to that over the fully allowed one using the phenomenological amplitudes of the experimental analyses. They are equal to 0.71 in the case of the $\rho(770)^0$ and a $m_{\pi\pi}$ range 0.66–0.90 GeV and to 0.69 for the $f_0(980)$ which dominates in the 0.90–1.06 GeV range. In fitting our model to the data, these coefficients reduce the branching fractions and their errors by the same factor.

Experimental cuts on the effective pion-kaon mass influence the $\pi\pi$ effective-mass and the helicity-angle distributions. A typical veto cut is experimentally used around the $K\pi$ effective mass, close to the D-meson mass. In our calculations, we have applied the cuts specified by the Belle and *BABAR* collaborations in their analyses of the B decays into $\pi\pi K$.

Our model has four complex parameters: P_u and P_t in the P-wave amplitude and S_u and S_t in the S-wave amplitude. With these parameters we shall describe more than 200 data values.

V. RESULTS

We have performed a global fit to the available data measured by *BABAR* and Belle. These consist of 204 data points describing the $\pi\pi$ mass and angular distributions and of 18 observables enumerated in Sec. IV. The χ^2 values are the following: $\chi^2_{\rm I}/W_{\rm I} = 9.8$ and $\chi^2_{\rm II} = 336.3$. The values of the eight real parameters are listed in Table I along with the parabolic errors from the MINUIT minimization procedure [27].

In Table II, the values of branching fractions, direct and time-dependent CP asymmetries are presented along with the corresponding experimental ones. The calculated observables for a given channel are integrated over the $m_{\pi\pi}$ range indicated in this table. Both the *BABAR* and Belle values are in agreement within their error bars and are well reproduced in our model. The theoretical errors stem from the parameter errors given in Table I.

In Secs. V A and V B, we present the $\pi\pi$ mass and helicity-angle distributions for charged and neutral $B \to \pi^+\pi^- K$ decays, respectively. Interference effects are studied in Sec. V C and some discussion on the results is given in Sec. V D.

A. The $\pi\pi$ mass and helicity-angle distributions in $B^0 \to \pi^+\pi^- K^0_S$ decays

In Fig. 2 the $\pi\pi$ effective-mass distributions of our model are compared to the Belle data [23]. In the fit to these distributions, the background corrected data have been used. One sees from Figs. 2(a) and 2(b) that our model describes rather well the $\pi^+\pi^-$ spectra measured by the Belle Collaboration separately for the B^+ and B^- decays. Our theoretical curve depicts, as in previous work [7], a prominent maximum near 1 GeV, to which now adds a less pronounced peak at about 770–780 MeV. Remarkably, one observes a clearly visible asymmetry in a number of events between the $B^- \to K^-\pi^+\pi^-$ and $B^+ \to K^+\pi^+\pi^-$ decays for the $\rho(770)^0$ and $f_0(980)$ regions. At lower $m_{\pi\pi}$ masses about 500 MeV, our model also produces a broad maximum which we attribute to the σ or $f_0(600)$. By the same token, we note that in fits to their data, the Belle Collaboration has not included the σ reso-

TABLE I. Charming penguin parameters in the S wave (S_u and S_t) and in the P wave (P_u and P_t).

Parameter	Value
$\lvert S_u\rvert$	0.15 ± 0.10
$\arg S_u$	1.90 ± 0.71
$\lvert S_t\rvert$	0.020 ± 0.002
$\arg S_t$	-0.26 ± 0.21
$\lvert P_u\rvert$	1.09 ± 0.21
$\arg P_u$	-0.98 ± 0.12
$\lvert P_t\rvert$	0.065 ± 0.002
$\arg P_t$	-1.56 ± 0.08

TABLE II. Average branching fractions $\mathcal{B}$ in units of 10^{-6}, asymmetries $\mathcal{A}_{CP}$, and the asymmetry parameters $\mathcal{S}$ and $\mathcal{A}$ of our model compared to the values of Belle and *BABAR* collaborations. The experimental branching ratios and their errors have been multiplied by 0.71 for $B \to \rho K$ channels and by 0.69 for $B \to f_0 K$ channels (for explanation see Sec. IV).

Observable	Channel	$\pi^+\pi^-$ mass range (GeV)	Our model	Belle	Ref.	*BABAR*	Ref.
$\mathcal{B}$	$\rho^0 K^\pm$	(0.66, 0.90)	2.91 ± 0.10	2.76 ± 0.45	[1]	3.60 ± 0.71	[4]
$\mathcal{A}_{CP}$	$\rho^0 K^\pm$	(0.66, 0.90)	0.32 ± 0.03	0.30 ± 0.14	[1]	0.32 ± 0.16	[4]
$\mathcal{B}$	$f_0 K^\pm$	(0.90, 1.06)	6.93 ± 0.16	6.06 ± 1.08	[1]	6.53 ± 0.85	[4]
$\mathcal{A}_{CP}$	$f_0 K^\pm$	(0.90, 1.06)	0.02 ± 0.02	-0.08 ± 0.08	[1]	0.09 ± 0.12	[4]
$\mathcal{B}$	$\rho^0 K^0$	(0.66, 0.90)	3.49 ± 0.20	4.35 ± 1.05	[3]	3.62 ± 1.14	[5]
$\mathcal{B}$	$f_0 K^0$	(0.90, 1.06)	3.86 ± 0.14	5.24 ± 1.28	[3]	3.79 ± 0.62	[5]
$\mathcal{S}$	$\pi^+\pi^- K_S^0$	(0.66, 0.90)	0.11 ± 0.11	–		0.17 ± 0.58	[26(a)]
$\mathcal{A}$	$\pi^+\pi^- K_S^0$	(0.66, 0.90)	0.01 ± 0.06	–		-0.64 ± 0.48	[26(a)]
$\mathcal{S}$	$\pi^+\pi^- K_S^0$	(0.89, 1.088)	-0.67 ± 0.05	-0.47 ± 0.37	[24(a)]		
$\mathcal{S}$	$\pi^+\pi^- K_S^0$	(0.86, 1.10)	-0.63 ± 0.05			-0.95 ± 0.29	[25]
$\mathcal{A}$	$\pi^+\pi^- K_S^0$	(0.89, 1.088)	-0.11 ± 0.07	-0.23 ± 0.26	[24(a)]		
$\mathcal{A}$	$\pi^+\pi^- K_S^0$	(0.86, 1.10)	-0.11 ± 0.07			0.24 ± 0.34	[25]

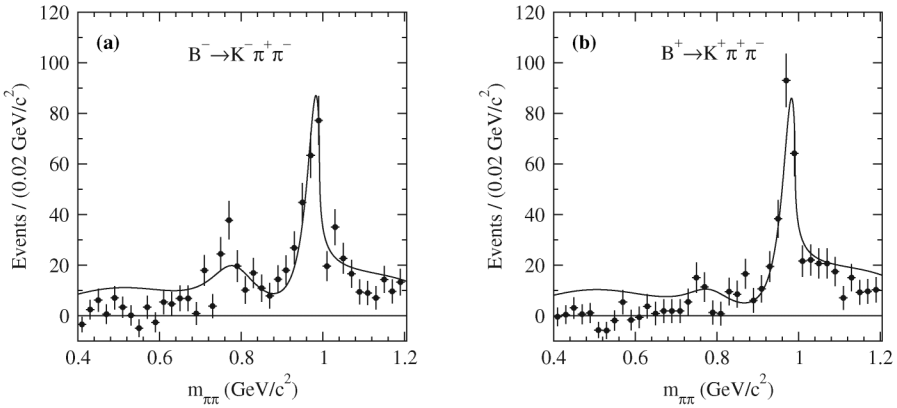

FIG. 2. The $\pi^+\pi^-$ effective-mass distributions (a) in $B^- \to \pi^+\pi^- K^-$ and (b) in $B^+ \to \pi^+\pi^- K^+$ decays. The data are taken from the Belle Collaboration [23]. The solid lines represent the results of our model.

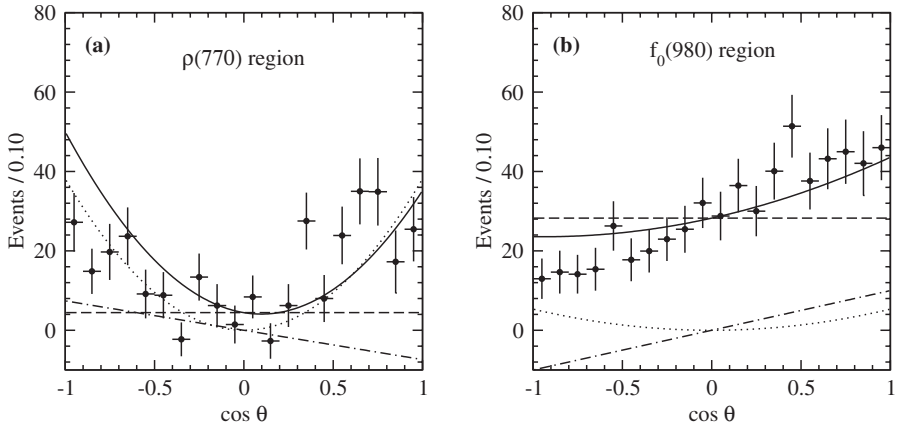

FIG. 3. Helicity-angle distributions in $B^\pm \to \pi^+\pi^- K^\pm$ (a) in the $\rho(770)$ mass region ($0.6\ \text{GeV} < m_{\pi\pi} < 0.9\ \text{GeV}$) and (b) in the $f_0(980)$ region ($0.9\ \text{GeV} < m_{\pi\pi} < 1.06\ \text{GeV}$). The data points are from Ref. [23] and the solid lines denote our model. The S-wave contribution is plotted with dashed lines, the P wave with dotted lines and the interference term with dotted-dashed lines.

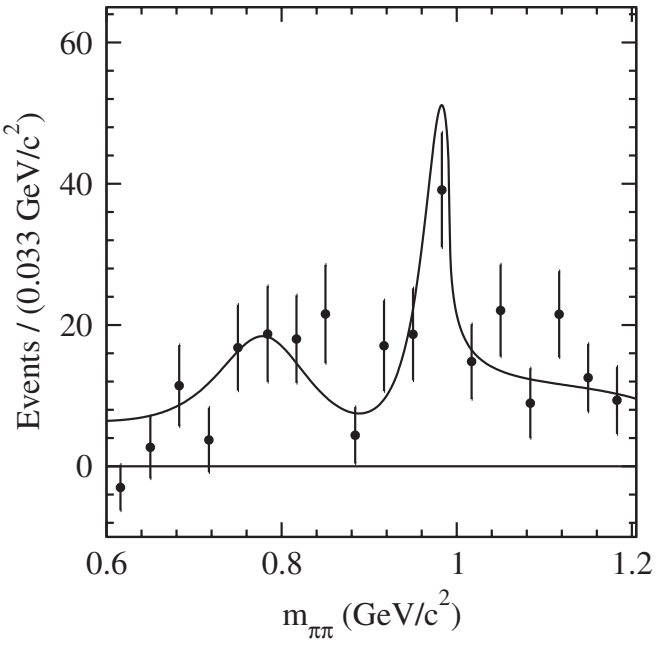

FIG. 4. The $\pi^+\pi^-$ effective-mass distributions in $B^0 \to \pi^+\pi^- K^0_S$ decays. Data points are taken from the *BABAR* Collaboration [5] while the continuous line results from our model.

nance which is thus buried in the nonresonant background. Let us remark that this part of the $m_{\pi\pi}$ spectrum has not been fitted in our calculations. As explained in Sec. IV, we have intentionally chosen the lower mass limit to be equal to 0.6 GeV.

In Fig. 3, we compare the results of our model for the $\cos\theta$ distribution in the vicinity of the $\rho(770)^0$ [Fig. 3(a)] and of the $f_0(980)$ [Fig. 3(b)] with the Belle data [23]. The experimental $\cos\theta$ distribution is fairly well reproduced given the fluctuation in events of the data points. The behavior of the angular distribution such as seen near the $f_0(980)$ mass is typical for a substantial interference pattern between the S and P wave. The former gives a constant contribution while the latter is a symmetric $\cos^2\theta$ distribution observed in the $\rho(770)^0$ mass range [see Eq. (22)]. The $S-P$ interference term, which is proportional to $\cos\theta$, is clearly seen in Fig. 3(b). This demonstrates the presence of the P-wave contribution in the $f_0(980)$ region.

B. The $\pi\pi$ mass and helicity-angle distributions in $B^0 \to \pi^+\pi^- K^0$ decays

The $m_{\pi\pi}$ effective-mass distribution for neutral B decays is plotted in Fig. 4 along with the results obtained by *BABAR* [5]. Within the error bars our model also describes this $m_{\pi\pi}$ distribution well, which bears the same features concerning the $\rho(770)^0$ and $f_0(980)$ as the charged B decay $m_{\pi\pi}$ spectrum. In Fig. 5(a) and 5(b) the $\cos\theta$ distributions in the proximity of the $\rho(770)^0$ and $f_0(980)$ are compared with the experimental data from Belle [3]. While the $\rho(770)^0$ range is dominated by the P-wave contribution, in the $f_0(980)$ range one observes once again the interference pattern. The sign of the interference term is, however, opposite to that apparent in Fig. 2(b). It is well explained by our model in which the P-wave and S-wave amplitudes for both charged and neutral B decays are closely related [see Eqs. (3) and (10) where the signs of the charming penguin terms are reversed].

C. Interference effects

In this subsection we study the interplay between the S and P waves of the decay amplitudes. Figure 6 shows the angular dependence of the two CP-violating asymmetries $\mathcal{S}$ and $\mathcal{A}$ calculated at the effective masses $m_{\pi\pi} = 775.8$ MeV and $m_{\pi\pi} = 980$ MeV using Eqs. (28a), (28b), and (29). These numbers are chosen to demonstrate the behavior of the asymmetries about the $\rho(770)^0$ and $f_0(980)$ resonances. As seen in Fig. 6(a) and 6(b), the functions $\mathcal{S}$ and $\mathcal{A}$ are not constant. This is a clear demonstration of the interference between S and P waves. The sharp changes in behavior of the asymmetry $\mathcal{S}$ at the $\rho(770)^0$ mass are shown in Fig. 6(c), where the straight dashed and dotted lines are the $\mathcal{S}$ values for separate S- and P-wave contributions, respectively. At $\cos\theta = 0$, the

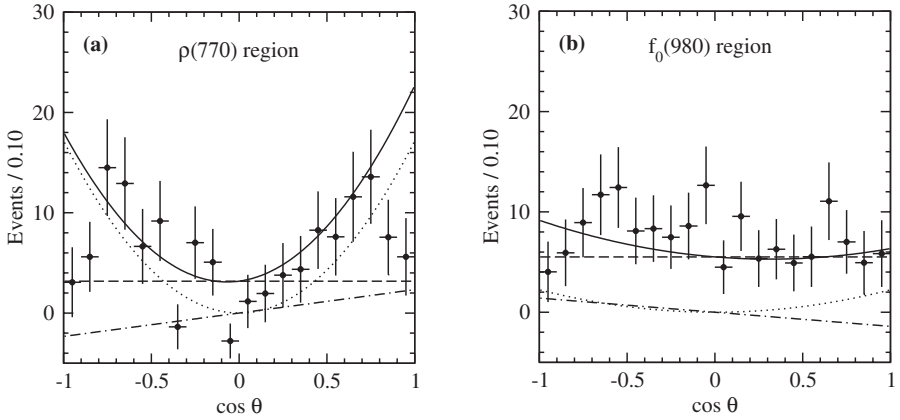

FIG. 5. As in Fig. 2 but for $B^0 \to \pi^+\pi^- K^0_S$ decays and for data from Belle [3].

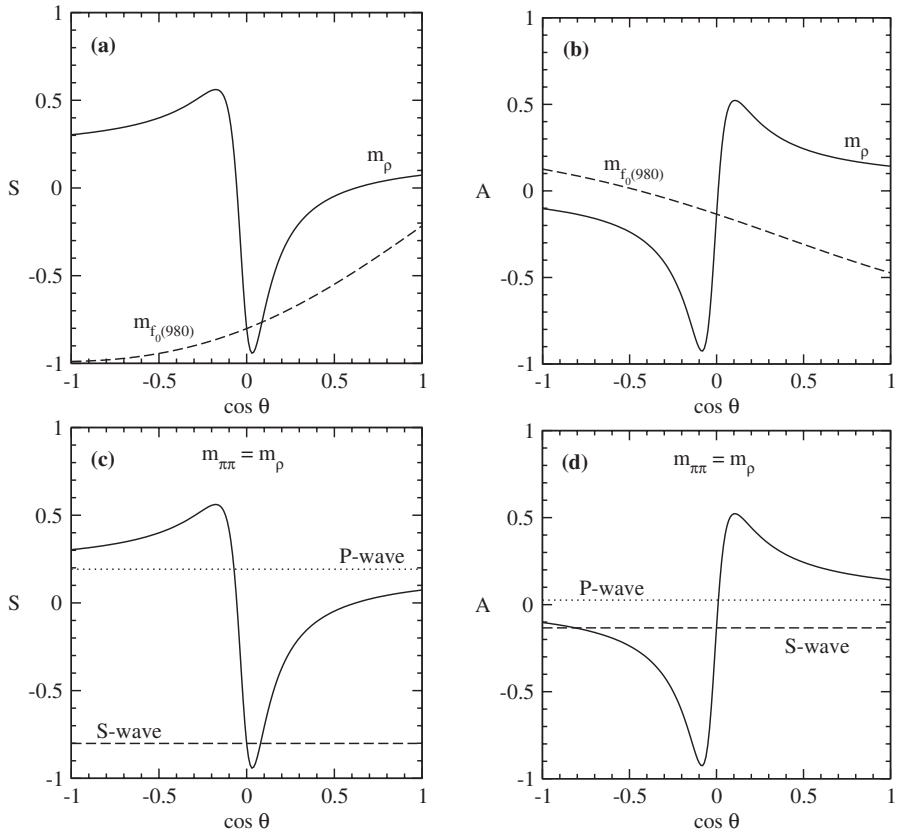

FIG. 6. Helicity-angle dependence of the CP-violating asymmetries $\mathcal{S}$ and $\mathcal{A}$ calculated for $B^0 \to \pi^+\pi^- K_S^0$ decays at $m_{\pi\pi}$ equal to $m_\rho = 775.8$ MeV [solid lines in (a)–(d)] and to $m_{f_0(980)} = 980$ MeV [dashed lines in (a) and (b)]. Separate S-wave (dashed lines) and P-wave results (dotted lines) are shown in (c) and (d) for $m_{\pi\pi} = m_\rho$.

P-wave amplitude vanishes, therefore the strongest variations of the asymmetry are observed near $\theta = \pi/2$. A similar picture for the asymmetry $\mathcal{A}$ is shown in Fig. 6(d).

The asymmetries $\mathcal{S}$ and $\mathcal{A}$ at $m_{\pi\pi} = 980$ MeV behave smoothly near $\cos\theta = 0$ since there the S wave dominates. A decrease of $\mathcal{A}$ as well as an increase of $\mathcal{S}$ as functions of $\cos\theta$ are due to the P-wave amplitude component, which is still nonnegligible in the $f_0(980)$ mass range.

Recall that the helicity-angle dependence of the asymmetries can be transformed into the functional dependence on the $\pi^- K$ effective mass

$$m_{\pi^- K} = \sqrt{m_\pi^2 + M_K^2 + m_{\pi\pi}E_K(m_{\pi\pi}) + 2|\mathbf{p}_\pi||\mathbf{p}_K|\cos\theta}, \tag{35}$$

where m_π is the pion mass. Thus, the above interference effects also can be experimentally studied by examination of particular regions of the Dalitz plot.

In Fig. 7, the effective $\pi\pi$ mass dependence of the asymmetries integrated over $\cos\theta$ are plotted [see Eqs. (30) and (31)]. The most pronounced effect is an intermediate change of sign of $\mathcal{S}$ near the $\rho(770)^0$ resonance. We stress that if the S- or P-amplitudes were dominated by only one weak amplitude proportional to λ_t then the asymmetry $\mathcal{S}$ shown in Fig. 7(a) would suddenly jump from $-\sin 2\beta \approx -0.7$ at the $\pi\pi$ threshold to $+\sin 2\beta \approx +0.7$ near the $\rho(770)^0$ mass and abruptly drop down to $-\sin 2\beta \approx -0.7$ at the $f_0(980)$ mass, as can be inferred from Eq. (30). A smooth behavior of $\mathcal{S}$ is explained by the mass dependence of the S-wave scalar form factors and by the finite width of the $\rho(770)^0$. As seen in Fig. 7(a), our model is in agreement with the data. Remarkably, there is a particularly large departure from the $+\sin 2\beta$ value near the $\rho(770)^0$ mass. This can be explained by a substantial value of the weak part of the amplitude in Eqs. (6) and (10) proportional to λ_u. In this context, bear in mind that the P-wave penguin parameter $|P_u|$ is much larger than the S-wave parameter $|S_u|$ (see Table I).

The functional dependence of the asymmetry $\mathcal{A}$ on $m_{\pi\pi}$ is depicted in Fig. 7(b). It is not as strong as for the $\mathcal{S}$ asymmetry, but certainly $\mathcal{A}$ is not equal to zero. In the $f_0(980)$ range, $\mathcal{A}$ is close to -0.1. Hence, it is comparable to the values of $\mathcal{A}$ found by Belle and *BABAR* in $B^0 \to K^+\pi^-$ decays [28,29]. In the former case, however, the experimental errors are yet too large to claim the nonzero value of $\mathcal{A}$ (see Table II).

We conclude this section by remarking that in penguin dominated decays, such as $B \to \rho K, \omega K \ldots$, tree diagrams are either CKM suppressed or CKM and color suppressed.

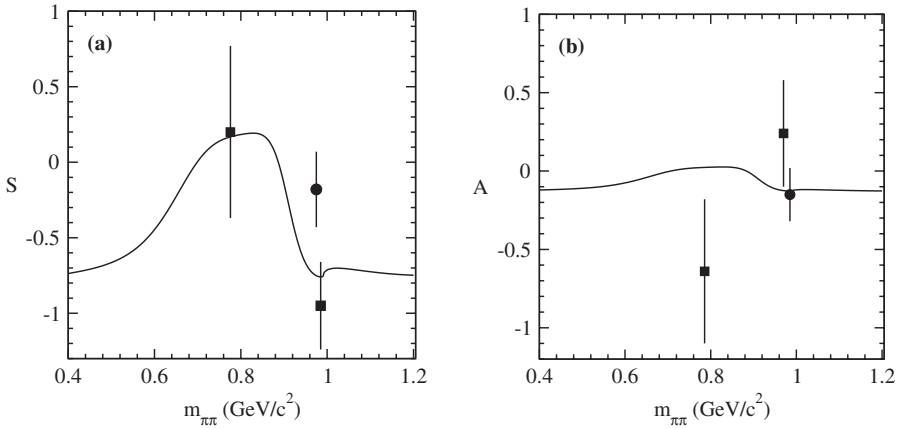

FIG. 7. Effective-mass dependence of the *CP*-violating asymmetries, integrated over $\cos\theta$, $\mathcal{S}$ in (a) and $\mathcal{A}$ in (b) obtained with our model (solid lines). The Belle Collaboration results [24(b)] for the $f_0(980)$ resonance are plotted as circles and the *BABAR* data for the $f_0(980)$ [25] and $\rho(770)^0$ [26(b)] as squares.

Still, we observe that for $\rho(770)^0 K$ final states an accidental cancellation occurs in the λ_u terms of Eqs. (4) and (11) due to the combinations $a_4^c - r a_6^c$ and $a_4^u - r a_6^u$, where $r \simeq 1$, $a_6^{u,c} \approx a_4^{u,c}$. A similar cancellation takes equally place in the $B \to f_0(980)K$ channel [7]. Therefore, the "tree pollution" is considerable and one may, at this point already, expect deviations from the value $\mathcal{S} \approx \sin 2\beta$ associated with the pure tree diagram for the $B^0 \to J/\psi K_S$ or with the penguin diagram for the $B^0 \to \phi K^0$ decays. The tree diagram contribution to the $\rho(770)^0 K$ state, however, is not sufficient to explain the important departure of $\mathcal{S}$ from the above value. It is the aforementioned long-distance contribution $|P_u|$ to the λ_u term combined with interference effects that determine the functional behavior of the $\mathcal{S}$ asymmetry parameter.

D. Discussion of the results

We stress the importance of charming penguin terms. Without them it is not possible to obtain a good agreement of the theoretical branching ratios with experimental data. If all the penguin parameters are set equal to zero then the model branching ratio is underestimated by a factor of about 5 for the $B^0 \to f_0(980)K^0$ decay and by 3.5 for the $B^0 \to \rho(770)^0 K^0$ decay. For the charged B decays the theoretical branching ratios are too small by factors of about 2.4 and 7 for the $f_0(980)K$ and $\rho(770)^0 K$ channels, respectively.

It has, however, been found in Ref. [10] that the branching ratios for $B \to f_0(980)K$ decays can be reproduced in the QCD factorization approach provided that one uses a large scalar decay constant $f_{f_0}^s$ of 370 MeV. The work of Ref. [10] is based on a two-body B-decay amplitude. Our approach considers a three-body B-decay amplitude by taking into account the $f_0(980)$ disintegration into two pions or two kaons and also by introducing final-state interactions between them. A relation between the two- and three-body B-decay amplitudes, elucidated in the appendix, leads in our case to a value of 94 MeV for $f_{f_0}^s$ as seen in Eq. (A14). The difference with the value of Ref. [10] by a factor of about 4 explains partly why we underestimate the $B \to f_0(980)K$ branching ratio if long-distance charming penguin contributions are absent.

We have studied the sensitivity of our results on the scalar form factors $\Gamma_{i=1,2}^{n,s}(m_{\pi\pi})$ which depend on the not very well known low-energy constants of the chiral perturbation theory. The possible variation of their values (see Refs. [20,30]) can lead up to a multiplicative factor of about 1.25 for $\Gamma_{i=1,2}^{n,s}(m_{\pi\pi})$ in the $f_0(980)$ range. Note however, that the sensitivity to such changes is limited due to the constant value of the product $\chi|\Gamma_1^n(m_{f_0})|$ given by Eq. (A15). If, for example, $\Gamma_1^n(m_{f_0})$ is multiplied by a factor of 1.25, the χ value is to be divided by 1.25 and consequently the value of $f_{f_0}^s$ is also multiplied by 1.25 [see Eq. (A14)]. Thus, an increase of the scalar form factor $\Gamma_1^s(m_{f_0})$ will only enhance the contribution of the $Q(m_{\pi\pi})V$ term in Eq. (A12).

Our $B \to (\pi\pi)_S K$ amplitude depends also on the $F_0^{B\to(\pi\pi)_S}(M_K^2)$ transition form factor which is a model-dependent quantity. Decreasing its value from 0.46 (see Sec. II C) to 0.25 (value quoted in Ref. [10]) will lead to a readjustment of the charming parameters S_u and S_t while fitting the experimental data. The quality of the fit is good and similar to that presented here. We also have obtained a good fit using the values of the low-energy constants determined in Ref. [30] (the values of the first line of Table I therein) for the scalar form factors together with $F_0^{B\to(\pi\pi)_S}(M_K^2) = 0.25$. Our conclusions are not changed by these possible modifications of our input.

VI. CONCLUSIONS AND OUTLOOK

In our studies of $B \to \pi^+\pi^- K$ decays, we have extended the work of Ref. [7] by adding the P-wave contribution to that of the S wave in the two-pion final-state

interactions. The total amplitude contains the resonant channels $B \to \rho(770)^0 K$ and $B \to f_0(980)K$. This work goes beyond the usual approach of calculating two-body branching ratios of the B decays, as we have taken into account parts of the final-state interactions between particles in three-body decay channels. In this paper, we have analyzed the interactions between pairs of pions in the Dalitz plot section with the $\pi\pi$ effective-mass range from threshold to about 1.2 GeV. In the S wave the rescattering or the transition amplitudes between two pions or two kaons are described by the unitary coupled-channel model of Ref. [19].

There are two components in the weak transition amplitudes. The first term is derived within the factorization approximation with some QCD corrections without hard-scattering and annihilation terms. The second contribution, called charming penguins, is a long-distance amplitude originating from penguin-type diagrams with c-quark or u-quark loops. Four complex charming penguin parameters, common for B^+, B^-, B^0, and $\bar{B}^0$ decays, have been introduced and fitted to numerous experimental data, including the $\pi\pi$ effective-mass and helicity-angle distributions, branching fractions, direct asymmetry $\mathcal{A}_{CP}$, and time-dependent CP-violating asymmetry parameters $\mathcal{S}$ and $\mathcal{A}$. Our theoretical model reproduces well the experimental results. Without the charming penguin amplitudes, the model branching fractions of $B \to f_0(980)K$ and $B \to \rho(770)^0 K$ decays are several times smaller than the experimental values. In the $m_{\pi\pi}$ range below 1.2 GeV, the two main resonances $\rho(770)^0$ and $f_0(980)$ give rise to important interference effects, best visible in the helicity-angle distributions. Thus, in Figs. 3 and 5, we notice sizable interference terms of opposite signs comparing the $B^\pm \to \pi^+\pi^- K^\pm$ decays with the $B^0 \to \pi^+\pi^- K^0$ ones.

In our model, the direct CP asymmetry in $B^\pm \to \rho^0 K^\pm$ decays is in agreement with the large experimental value measured by the Belle and *BABAR* groups. The parameter $\mathcal{S}$ of the time-dependent CP asymmetry for $B^0 \to \rho^0 K^0_S$ decays is significantly smaller than the value $\sin 2\beta$ expected in case of a full dominance of the weak decay amplitude proportional to λ_t. This is related to a large value of the u-penguin parameter P_u in the P wave (see Table I). The numbers S_u, S_t, P_u and P_t should be treated as phenomenological parameters which we attribute to the long-distance penguin contributions. In our opinion, however, they can also contain contributions from other processes omitted by us like annihilation or hard-spectator interaction terms.

In this approach, all the resonances appear in a natural way as poles of the meson-meson amplitudes. No arbitrary phases nor any relative intensity parameters for the two discussed resonances $\rho(770)^0$ and $f_0(980)$ are needed. This is in contrast to the usual phenomenological analyses in terms of the isobar model applied to fit the Dalitz plot density distributions. Let us remark that the scalar resonance $f_0(600)$, as a pole of the S-wave amplitude, is also present in the $\pi\pi$ effective-mass spectrum. However, it has not been included in the phenomenological models of the Belle and *BABAR* Collaborations [2,4,23].

So far, we have restricted our analysis to an effective $\pi\pi$ mass of about 1.2 GeV. In further studies, one can extend not only this mass range to include further scalar and vector resonances but also treat the other variable $m_{\pi K}$ on the Dalitz plot and the accompanying vector resonances K^*. Given our findings for the $f_0(980)$ and $\rho(770)^0$ resonances, we expect many more interference effects at larger effective $\pi\pi$ masses and also for the πK effective-mass range.

ACKNOWLEDGMENTS

One of us (L. L.) is very grateful to Maria Różańska for many useful conversations and remarks on B-meson decays. B. E. is thankful to Thomas Latham for providing access to the *BABAR* raw data on effective-mass distributions including background corrections. B. E. and B. L. acknowledge pleasant and helpful discussions with José Ocariz and also thank Olivier Leitner for quite useful comments. This work has been performed within the framework of the IN2P3-Polish Laboratories Convention (Project No. CSI-12). A visit of B. E. in Kraków has been partly financed within an agreement between the CNRS (France) and the Polish Academy of Sciences (Project No. 19481). B. E. is supported by a Marie Curie International Reintegration Grant under the Contract No. 516228.

APPENDIX: AMPLITUDES FOR THE $B^- \to f_0(980)K^-$ AND $B^- \to (\pi^+\pi^-)_S K^-$ DECAYS

We give here the expressions for the two-body $\langle f_0 K^- | H | B^- \rangle$ and the three-body $\langle (\pi^+\pi^-)_S K^- | H | B^- \rangle$ decay amplitudes and show how they are related to each other. In the QCD factorization approach, adding charming penguin terms, the former amplitude can be written as

$$\langle f_0 K^- | H | B^- \rangle = \frac{G_F}{\sqrt{2}} [P(m_{f_0})U + C^S(m_{f_0}) + \bar{Q}(m_{f_0})V + C^S(M_K)]. \quad \text{(A1)}$$

If electroweak penguin and annihilation terms are not included,

$$P(m_{f_0}) = f_K(M_B^2 - m_{f_0}^2) F_0^{B\to f_0}(M_K^2), \quad \text{(A2)}$$

$$\bar{Q}(m_{f_0}) = \frac{2\langle f_0 | \bar{s}s | 0 \rangle}{m_b - m_s} (M_B^2 - M_K^2) F_0^{B\to K}(m_{f_0}^2), \quad \text{(A3)}$$

$$U = \lambda_u [a_1 + a_4^u - a_4^c + (a_6^c - a_6^u) r] + \lambda_t (a_6^c r - a_4^c), \quad \text{(A4)}$$

$$V = \lambda_u(a_6^c - a_6^u) + \lambda_t a_6^c, \tag{A5}$$

where m_{f_0} is the $f_0(980)$ mass and $F_0^{B\to f_0}(M_K^2)$ and $F_0^{B\to K}(m_{f_0}^2)$ are the $B \to f_0(980)$ and $B \to K$ transition form factors. The scalar decay constant $f_{f_0}^s$ can be defined by the matrix element

$$\langle f_0|\bar{s}s|0\rangle = m_{f_0} f_{f_0}^s. \tag{A6}$$

The three-body decay amplitude reads

$$\begin{aligned}\langle(\pi^+\pi^-)_S K^-|H|B^-\rangle = \frac{G_F}{\sqrt{2}}\sqrt{\frac{2}{3}}\{&[P(m_{\pi\pi})U + C^S(m_{\pi\pi})]\\ &\times \Gamma_{f_0\pi\pi}^n(m_{\pi\pi})\\ &+ [\bar{Q}(m_{\pi\pi})V + C^S(M_K)]\\ &\times \Gamma_{f_0\pi\pi}^s(m_{\pi\pi})\},\end{aligned} \tag{A7}$$

where $\Gamma_{f_0\pi\pi}^n(m_{\pi\pi})$ and $\Gamma_{f_0\pi\pi}^s(m_{\pi\pi})$ are the nonstrange and strange vertex functions, respectively. They describe the decay of the $f_0(980)$ into two pions. The factor $\sqrt{2/3}$ is the Clebsch-Gordan coefficient which relates the isospin-0 S-wave $|(\pi\pi)_S\rangle$ to the $|(\pi^+\pi^-)_S\rangle$ one. The vertex function $\Gamma_{f_0\pi\pi}^s(m_{\pi\pi})$ is defined through the relation between the matrix elements

$$\langle(\pi\pi)_S|\bar{s}s|0\rangle = \Gamma_{f_0\pi\pi}^s(m_{\pi\pi})\langle f_0|\bar{s}s|0\rangle. \tag{A8}$$

Replacement of $\bar{s}s$ in Eq. (A8) by $\bar{n}n = \frac{1}{\sqrt{2}}(\bar{u}u + \bar{d}d)$ yields the corresponding $\Gamma_{f_0\pi\pi}^n(m_{\pi\pi})$ vertex function. The matrix element $\langle(\pi\pi)_S|\bar{s}s|0\rangle$ is related to the strange scalar form factor $\Gamma_1^s(m_{\pi\pi})$ by [20]

$$\langle(\pi\pi)_S|\bar{s}s|0\rangle = \sqrt{2}B_0\Gamma_1^{s*}(m_{\pi\pi}), \tag{A9}$$

where $B_0 = -\langle 0|\bar{q}q|0\rangle/f_\pi^2$ is proportional to the quark condensate, f_π being the pion decay constant. Let us note, by this occasion, that in Eq. (A9) the charge conjugation appears since the form factor Γ_1^s is defined as being proportional to the matrix element $\langle 0|\bar{s}s|(\pi\pi)_S\rangle$. One must also correct Eq. (11) of Ref. [7] in which $\Gamma_i^{n,s}$ should be replaced by $\Gamma_i^{n,s*}$. Using Eqs. (A6), (A8), and (A9) one finds

$$\Gamma_{f_0\pi\pi}^s(m_{\pi\pi}) = \chi\Gamma_1^{s*}(m_{\pi\pi}), \tag{A10}$$

where the constant χ is defined by

$$\chi = \frac{\sqrt{2}B_0}{m_{f_0} f_{f_0}^s}. \tag{A11}$$

We assume $\Gamma_{f_0\pi\pi}^n(m_{\pi\pi})$ to be related to the nonstrange scalar for factor $\Gamma_1^{n*}(m_{\pi\pi})$ by the same constant χ as in Eq. (A10). Here, $\Gamma_1^{n*}(m_{\pi\pi}) = \langle(\pi\pi)_S|\bar{n}n|0\rangle/\sqrt{2}B_0$ similarly to Eq. (A9). Making the appropriate replacements for $\Gamma_{f_0\pi\pi}^s(m_{\pi\pi})$ and $\Gamma_{f_0\pi\pi}^n(m_{\pi\pi})$ in Eq. (A7), we finally arrive at

$$\begin{aligned}\langle(\pi^+\pi^-)_S K^-|H|B^-\rangle = \frac{G_F}{\sqrt{2}}\sqrt{\frac{2}{3}}\{&\chi[P(m_{\pi\pi})U + C^S(m_{\pi\pi})]\\ &\times \Gamma_1^{n*}(m_{\pi\pi})\\ &+ [Q(m_{\pi\pi})V + \chi C^S(M_K)]\\ &\times \Gamma_1^{s*}(m_{\pi\pi})\},\end{aligned} \tag{A12}$$

where the relation

$$Q(m_{\pi\pi}) = \bar{Q}(m_{\pi\pi})\chi \tag{A13}$$

holds. Thus, Eq. (A12) is identical to Eq. (1) of Ref. [7]. From Eq. (A11) it follows

$$f_{f_0}^s = \frac{\sqrt{2}B_0}{m_{f_0}\chi}. \tag{A14}$$

With $\chi = 29.8\ \text{GeV}^{-1}$, $B_0 = m_\pi^2/2\hat{m}$ and $\hat{m} = 5$ MeV, $m_{f_0} = 980$ MeV one obtains $f_{f_0}^s = 94$ MeV. In our model $f_{f_0}^s$ is determined by the $f_0(980)$ properties since [7]

$$\chi = \frac{g_{f_0\pi\pi}}{m_{f_0}\Gamma_{\text{tot}}(f_0)}\frac{1}{|\Gamma_1^n(m_{f_0})|}. \tag{A15}$$

Here $\Gamma_{\text{tot}}(f_0)$ is the total $f_0(980)$ width. The constant χ enters in the description of the decay of the scalar resonances into two pions as seen from Eq. (A10) and comments below Eq. (A11). Furthermore Eq. (A15) shows that χ has the same role as the coupling constant $g_{\rho\pi\pi}$ of Eq. (14).

As can be seen from Eqs. (A1) and (A6) the two-body part of QCD factorization amplitude without charming penguins is similar to the corresponding one of Ref. [10] when excluding electroweak penguin and annihilation contributions. Note, however, that we disagree with the relative sign between the $P(m_{\pi\pi})U$ [Eqs. (A2) and (A4)] and $Q(m_{\pi\pi})V$ [Eqs. (A3) and (A5)] terms. Our relative sign agrees with that of Ref. [31].

[1] A. Garmash *et al.* (Belle Collaboration), Phys. Rev. Lett. **96**, 251803 (2006).

[2] A. Garmash *et al.* (Belle Collaboration), Phys. Rev. D **71**, 092003 (2005).

[3] K. Abe *et al.* (Belle Collaboration), hep-ex/0509047.
[4] B. Aubert *et al.* (*BABAR* Collaboration), Phys. Rev. D **72**, 072003 (2005).
[5] B. Aubert *et al.* (*BABAR* Collaboration), Phys. Rev. D **73**, 031101(R) (2006).
[6] B. Aubert *et al.* (*BABAR* Collaboration), hep-ex/0408079.
[7] A. Furman, R. Kamiński, L. Leśniak, and B. Loiseau, Phys. Lett. B **622**, 207 (2005).
[8] M. Ciuchini, E. Franco, G. Martinelli, and L. Silvestrini, Nucl. Phys. **B501**, 271 (1997).
[9] H. Y. Cheng, C. K. Chua, and A. Soni, Phys. Rev. D **71**, 014030 (2005); **72**, 014006 (2005).
[10] H. Y. Cheng, C. K. Chua, and K. C. Yang, Phys. Rev. D **73**, 014017 (2006).
[11] C. M. Arnesen, Z. Ligeti, I. Z. Rothstein, and I. W. Stewart, hep-ph/0607001.
[12] Ch. W. Bauer, D. Pirjol, I. Z. Rothstein, and I. W. Stewart, Phys. Rev. D **70**, 054015 (2004).
[13] M. Beneke, G. Buchalla, M. Neubert, and C. T. Sachrajda, Phys. Rev. D **72**, 098501 (2005).
[14] O. Leitner, X. H. Guo, and A. W. Thomas, J. Phys. G **31**, 199 (2005).
[15] M. Beneke and M. Neubert, Nucl. Phys. **B675**, 333 (2003).
[16] G. Buchalla, G. Hiller, Y. Nir, and G. Raz, J. High Energy Phys. 09 (2005) 074.
[17] M. Beneke, Phys. Lett. B **620**, 143 (2005).
[18] N. de Groot, W. N. Cottingham, and I. B. Whittingham, Phys. Rev. D **68**, 113005 (2003).
[19] R. Kamiński, L. Leśniak, and B. Loiseau, Phys. Lett. B **413**, 130 (1997).
[20] U. G. Meissner and J. A. Oller, Nucl. Phys. **A679**, 671 (2001).
[21] M. Beneke, G. Buchalla, M. Neubert, and C. T. Sachrajda, Nucl. Phys. **B606**, 245 (2001).
[22] J. Charles *et al.* (CKMfitter Group), Eur. Phys. J. C **41**, 1 (2005).
[23] K. Abe *et al.* (Belle Collaboration), hep-ex/0509001.
[24] (a) K. Abe *et al.* (Belle Collaboration), hep-ex/0507037; (b) K. Abe*et al.* (Belle Collaboration), hep-ex/0609006.
[25] B. Aubert *et al.* (*BABAR* Collaboration), hep-ex/0408095.
[26] (a) *BABAR* Collaboration, cited by Heavy Flavor Averaging Group, 2006 (unpublished); (b) B. Aubert *et al.* (*BABAR* Collaboration), hep-ex/0608051.
[27] F. James and M. Roos, Comput. Phys. Commun. **10**, 343 (1975).
[28] B. Aubert *et al.* (*BABAR* Collaboration), Phys. Rev. Lett. **93**, 131801 (2004).
[29] K. Abe *et al.* (Belle Collaboration), hep-ex/0507045.
[30] T. A. Lähde and U. G. Meißner, Phys. Rev. D **74**, 034021 (2006).
[31] D. Delepine, J. L. Lucio, and C. A. Ramirez, Eur. Phys. J. C **45**, 693 (2006).